A feasibility study into the robust control of a variable-frequency wide operating range flyback converter

Tue T. Vu[†], Seamus O'Driscoll[*] and John V. Ringwood[†]

[†]*Department of Electronic Engineering*
National University of Ireland, Maynooth

[*]*Texas Instrument Limited*
Cork, Ireland

E-mail: [†]ttrongvu@eeng.nuim.ie
[†]john.ringwood@eeng.nuim.ie

[*]seamusodriscoll@ti.com

Abstract — **Modelling and design of a robust controller for fixed-frequency PWM DC-to-DC power converters are well-known problems and have been intensively investigated in the literature. However, none of the existing studies considers the variable-frequency applications recently employed to improve efficiency. This paper focuses on synthesizing a robust compensator for a variable-frequency, wide operating range, flyback converter using the H_∞ framework. The simulation results show that it is possible to design a single controller that can preserve stability over the whole working range of the converter, but robust performance may be compromised.**

Keywords — **Robust H_∞ control, flyback conveter, variable frequency PWM.**

I Introduction

In the field of AC-to-DC external power supplies, a single stage flyback converter, as illustrated in Fig. 1, is a primary candidate for low-power applications, due to its inherently simple structure and cost-effective nature. Owing to the urgent demand for energy saving, various techniques have been recently proposed to reduce the losses occurring inside flyback converters [1, 2]. Due to the nature of these approaches, these converters usually have multi-operating modes and variable switching frequencies. Existing control methods for these multi-operating mode converters are heavily based on trial and error expertise [1, 2]. Though some studies claimed that their controllers are stable and provide good performance across all operating points [1], no theoretical proof has been provided so far. Therefore, this paper focuses on a systematic approach to the synthesis of a H_∞ robust compensator for a variable frequency, wide operating range, flyback converter.

The remainder of this paper is organized as follows. Section II conducts a systematic review of robust control for power converters, while the operating principle and small signal model of the flyback converter, as shown in Fig. 1, are briefly sketched in Section III. Based on the design framework and converter specifications, a robust controller is obtained in Section IV. The controller performance

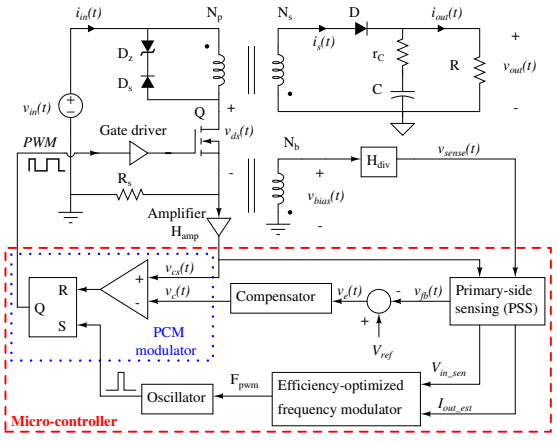

Fig. 1: Functional diagram of a variable frequency peak current mode (PCM) controlled flyback converter. For simplicity, the compensation ramp $i_a(t)$ for PCM is not included in this figure

analysis and conclusion are presented in Sections V and VI respectively.

II Robust control for power converters: a review

Designing a robust control that guarantees a stable operation and good performance, regardless of the plant uncertainty, has drawn attention from researchers in both academia and industry [3, 4, 5, 6]. In the field of power converters, such control strategies, e.g. H_∞ analysis, $\mu-$synthesis, etc., have been widely applied to various applications, ranging from buck-type to resonant-type converters.

The first H_∞ control for a DC-to-DC converter can be traced back to the publication of Naim *et al.*[7]. These authors applied H_∞ theory to stabilize the operation of a fixed switching frequency boost converter and simultaneously achieve good performance. Though the study showed interesting comparisons between robust control, current programmed control and feed forward control, the results are only valid for small deviations of the input voltage and output load from their nominal values. This limitation is due to the modelling approach used in [7], which simply considers the changes in the supply voltage and load current as exogenous signal disturbances rather than model uncertainty. Encouraged by the work of Naim *et al.* [7], other authors have subsequently extended the case study to different converter configurations [8, 9] and have improved many shortcomings in [7], such as the presence of non-zero steady state error and no experimental verification. However, the studies in [8, 9] still suffer from the small signal assumption of the model used and need to be applied with care for large signal variations.

In addition to the H_∞ robust approach, applications of μ-analysis in control design for power converters can be found in [10, 11, 12, 13, 14]. Particularly, Wang *et al.* [10] modelled parameter variations in a series resonant converter as input multiplicative perturbations, and employed the μ-synthesis procedure to obtain a robust controller. In a very similar manner, [11] presented a study for a parallel resonant converter while [12] demonstrated a robust design for a current-programmed controlled buck-boost converter. Since the effects of operating point movements were included in the models, the designs in [10, 11, 12] can satisfy both robust stability and performance over a wide range of operating conditions. The only concern is that the use of unstructured uncertainty, to describe the plant variations, can lead to a very conservative model and thus results in poor closed-loop performance. Addressing this limitation, Tymerski [13, 14] suggested using structured uncertainty to evaluate component tolerances in a DC-to-DC converter and representing the system equations in the $\Delta - M$ form, which is most convenient for structured singular value (μ) analysis. The comparisons in [14] show that, for the given set of parameter variations, the structured uncertainty modelling technique yields controllers which outperforms those returned by the unstructured uncertainty representation. Although it is more advantageous, in terms of achievable performance, to use structured uncertainty and μ-analysis as a control synthesis procedure for DC-to-DC converters [13, 14], certain types of perturbations, such as variations in the operating mode or in the switching frequency, could not be rearranged in the $\Delta - M$ form [15].

Other robust control techniques are also considered and applied to the area of PWM converters in [16, 17, 18, 19, 15]. For example, [16] makes use of the loop transfer recovery (LTR) methodology to obtain a compensator for a series parallel resonant converter, while, in [17], a combination of H_∞ and classical loop-shaping control is employed to enhance the transient response of a buck converter, as well as to ensure a robustly stable operation. Realizing the practical limitation of H_∞ and μ-analysis strategies, Olalla *et al.* [15] proposed an alternative control approach, based on Quantitative Feedback Theory (QFT), to tackle a wide change in parameters and operating mode of a buck converter. Experimental results of the QFT-based controller show good rejection to input voltage disturbances and output load variations, fast tracking of the reference signal, and stability under any excitation conditions. The applications of QFT to other converter topologies have carried out in [18, 19], but no experimental results are available.

In summary, modelling and design of a robust controller for fixed PWM frequency DC/DC power converters are well-known problems and have been intensively investigated in the literature. However, none of the existing studies considers the converter applications with a variable switching frequency. In this paper, the mixed-sensitivity H_∞ approach is applied to synthesize a robust compensator for a variable-frequency flyback converter.

III Small signal model of peak current mode flyback converter

The control design in Fig. 1 operates like traditional (peak current mode) PCM control, except that the switching frequency is variable, instead of fixed, and determined by the efficiency-optimized frequency modulator. The primary-side sensing (PSS) function provides the feedback signal for the compensator, and the input voltage and load current estimation for the efficiency-optimizer block.

For a broad external excitation and switching

frequencies, the flyback converter, as shown in Fig. 1, will operate in both continuous and discontinuous conduction modes (CCM and DCM), hence a small signal model of the converter, for each working scenario, is required. Since a peak current modulation is utilized in Fig. 1 to generate the PWM signal, the small signal model can be derived based on the principle as described in [20, 21]. Figure 2 shows a complete block diagram of the small signal model of both CCM and DCM flyback converters, taking into account the effects of the PSS function, voltage divider and current sense circuitry. In order to design the robust compensator $G_c(s)$, it is necessary to know the transfer functions of all blocks within the control loop.

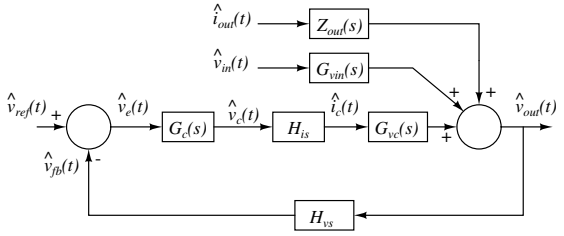

Fig. 2: Small signal model of the PCM controlled Flyback converter operating in both CCM and DCM.

It is assumed that the PSS function performs correctly and consistently, irrespective of the variations of the converter operating point. Therefore, the transfer function from the output voltage $v_{out}(t)$ to the feedback voltage $v_{fb}(t)$ in Fig. 1 can be simply modelled by

$$H_{vs} = \frac{\hat{v}_{fb}(t)}{\hat{v}_{out}(t)} = \frac{N_b}{N_s} H_{div}, \tag{1}$$

where N_s and N_b are the number of turns in the secondary and bias windings, respectively. H_{div} represents the voltage divider gain. The current sensing gain can be simply derived from the sense resistor R_s and current amplifier gain H_{amp} via

$$H_{is} = \frac{1}{H_{amp} R_s}. \tag{2}$$

For different working modes, the transfer function of the flyback converter, i.e. $G_{vc}(s)$, will be different, so a separate derivation is required for each operating scenario.

a) $G_{vc}(s)$ in CCM

Using the state averaging method outlined in [20, 21], with an assumption that R_s is small and can be ignored and that all components are ideal, one can work out the transfer function $G_{vc}(s)$ in CCM as

$$G_{vc}(s) = \frac{\hat{v}_{out}(t)}{\hat{i}_c(t)} = \frac{F_m G_{vd}(s)}{1 + F_m \left(G_{id}(s) + F_v G_{vd}(s)\right)}, \tag{3}$$

where

$$G_{vd}(s) = \frac{\frac{V_{in}}{nL_mC}\left(1 - s\frac{n^2 D L_m}{(1-D)^2 R}\right)(1 + r_C C s)}{s^2 + \frac{n^2 L_m + R r_C C (1-D)}{n^2 R L_m C} s + \frac{(1-D)^2}{n^2 L_m C}},$$

$$G_{id}(s) = \frac{\frac{V_{out}(1+D)}{nDRL_mC}\left(1 + \frac{RC}{1+D} s\right)}{s^2 + \frac{n^2 L_m + R r_C C (1-D)}{n^2 R L_m C_o} s + \frac{(1-D)^2}{n^2 L_m C}},$$

$$F_m = \frac{1}{M_a T_{pwm}}, \qquad F_v = \frac{(1-D)^2 T_{pwm}}{2nL_m},$$

$$D = \frac{V_{out}}{V_{out} + nV_{in}}.$$

Recall that $n = \frac{N_s}{N_p}$ is the transformer turn ratio, M_a is the slope of the compensation ramp $i_a(t)$ and T_{pwm} indicates the period of the PWM signal. Capital letters V_{in}, V_{out} and D denote steady state values of signals at an operating point, while lower case symbols with a hat on them, such as $\hat{v}_{out}$, $\hat{i}_c$, *etc.*, represent signal deviations from their operating points.

b) $G_{vc}(s)$ in DCM

Similarly, the control signal $\hat{i}_c(t)$ to output voltage $\hat{v}_{out}(t)$ transfer function in DCM is given by

$$G_{vc}(s) = \frac{\hat{v}_{out}(t)}{\hat{i}_c(t)} = F_m G_{vd}(s) \tag{4}$$

where

$$G_{vd}(s) = \frac{2V_{in}}{nL_mC} \frac{\left(1 - \frac{DT_{pwm}}{2} s\right)}{s^2 + \left(\frac{1}{RC} + \frac{2M}{DT_{pwm}}\right) s + \frac{4M}{DT_{pwm}RC}}$$

$$M = D\sqrt{\frac{T_{pwm}R}{2n^2 L_m}}, \quad D = \frac{1}{\sqrt{\frac{T_{pwm}R}{2L_m}}} \frac{V_0}{V_{in}},$$

$$F_m = \frac{1}{\left(M_a + \frac{V_{in}}{L_m}\right) T_{pwm}}.$$

IV Robust controller design

In this paper, a 65W flyback converter design, whose parameters and working range are summarized in Table 1, is chosen as an example for our study. The synthesis of an H_∞ controller for such a system is described step-by-step in the next parts of this section.

a) Mixed-sensitivity H_∞ framework

The small signal model, presented in Section III, can predict the behaviour of the converter around a given operating point. However, there exist, in practice, several elements causing model/plant mismatches, such as low-order approximations, unmodelled dynamic, operating point movements,

Input voltage, V_{in}	120 - 373 V
Output voltage, V_{out}	19.5 V
Load resistance, R	$5.9 - 1950\Omega$
Switching frequency, F_{pwm}	1 - 120 kHz
Winding turns, $N_p : N_s : N_b$	26 : 6 : 4
Magnetizing inductance, L_m	$172\mu H \pm 20\%$
Output capacitance, C	$1390\mu F \pm 10\%$
Current sense resistor, R_s	$200m\Omega$
Voltage divider gain, H_{div}	0.165
Current amplifier gain, H_{amp}	4

Table 1: Component values and operating specifications of a 65W flyback converter.

etc.. These differences, usually referred as model uncertainty, greatly affect stability and performance of closed-loop systems, and hence are important for robust control. Generally, the model perturbation can be represented in a structured or unstructured manner. This study focuses on multiplicative unstructured uncertainty of the form [5]

$$G_p(s) = G(s)\left(1 + W_I(s)\Delta_I(s)\right), \tag{5}$$

where $G(s)$ denotes the nominal plant model with no uncertainty while $G_p(s)$ indicates the perturbed model. Here, $\Delta_I(s)$ is any stable transfer functions satisfying, $|\Delta_I(jw)| \leq 1\ \forall w$, and $W_I(s)$ is usually termed a multiplicative weight.

Given a set of model perturbations in Eq. (5), the mixed-sensitivity H_∞ framework seeks a controller $G_c(s)$ which minimizes the cost function [5]

$$\| F_l(P, G_c) \|_\infty = \left\| \begin{matrix} W_1(s)S(s) \\ W_2(s)T(s) \end{matrix} \right\|_\infty, \tag{6}$$

where $S(s) = (1 + G(s)G_c(s))^{-1}$ is the system sensitivity function, and $T(s) = G(s)G_c(s)\left(1 + G(s)G_c(s)\right)^{-1}$ is the complementary sensitivity function. The weighting functions $W_1(s)$ and $W_2(s)$ in Eq (6) are used as a means to specify the robustness and performance of the closed loop system. Particularly, $W_1(s)$ is chosen to reduce the sensitivity function $S(s)$ at low frequencies, i.e. good disturbance attenuation, and to ensure the robust performance for the perturbed plants through specifying the lowest performance bound. $W_2(s)$ is chosen to penalise the complementary sensitivity function $T(s)$ at high frequencies, i.e. good stability margin, and most importantly to achieve the robust stability by letting [5]

$$|W_2(jw)| \geq |W_I(jw)|, \qquad \forall w. \tag{7}$$

b) Model uncertainty

The frequency responses of $G_{vc}(s)$, at different combinations of the input voltage, output load and switching frequency, are plotted in Fig. 3. In order to yield the smallest uncertainty region, the nominal plant, as illustrated by the solid line in Fig. 3, is suggested as

$$G_{vcn}(s) = \frac{-343.244\left(s - 2.49 \cdot 10^6\right)}{(s + 57.56)\left(s + 8.093 \cdot 10^5\right)}. \tag{8}$$

Following the procedure in [5], one can easily obtain the magnitude of the relative uncertainty as shown in Fig. 4. In order to cover all this uncertainty, the second-order weight

$$W_I(s) = \frac{1.239(s + 0.8929)(s + 1000)}{(s + 1.212)(s + 1250)} \tag{9}$$

is used.

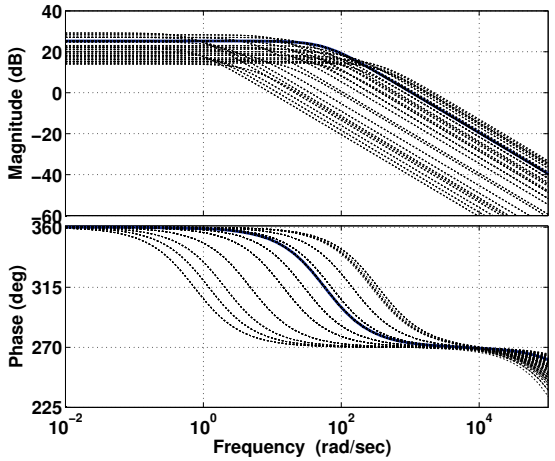

Fig. 3: Frequency response of G_{vc} at different working points. The solid line is the nominal plant while dotted lines are perturbed plants

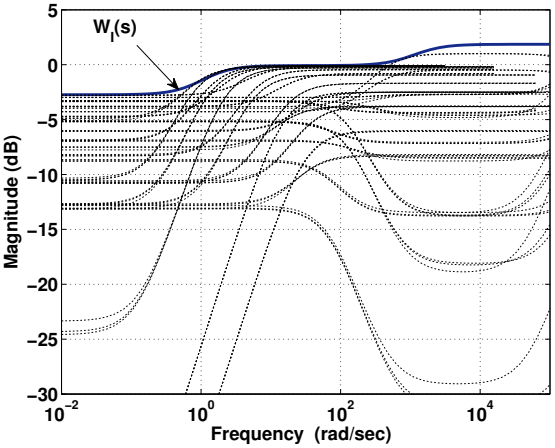

Fig. 4: Magnitude of the multiplicative uncertainty (dotted lines) for different working points and the uncertainty weight $W_I(s)$ (solid line)

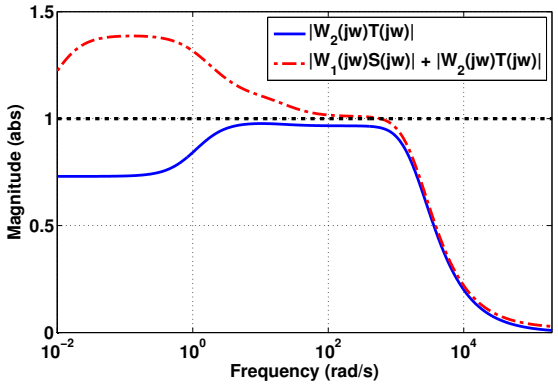

Fig. 5: Plots of $|W_2(jw)T(jw)|$ and $|W_1(jw)S(jw)| + |W_2(jw)T(jw)|$ for robust stability and performance assessment. The upper boundary to guarantee the robustness is 1.

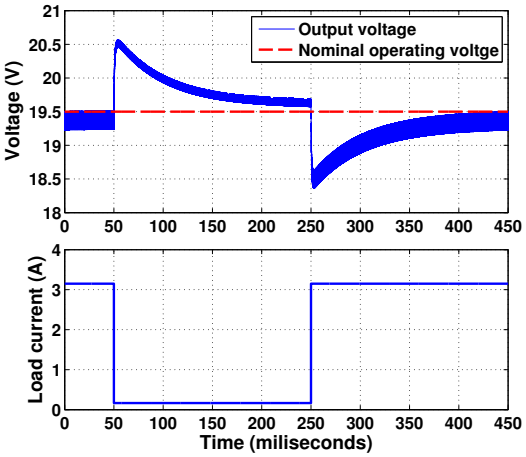

Fig. 6: Variation of the converter output voltage in response to a dynamic load stepping between $0.165A$ and $3.15A$ every 200 milliseconds. The input voltage V_{in} is kept fixed at 150V.

c) Weight selection

Some performance specifications, i.e. the tracking/regulation error and closed-loop bandwidth, can be achieved by means of the weight $W_1(s)$. In particular, the weight $W_1(s)$ must act like an integrator at low frequencies to achieve zero steady-state error, while moving the zero crossing point of $W_1(s)$ to higher frequencies can help to increase the bandwidth of the closed-loop system. Based on such observation, $W_1(s)$ is chosen as

$$W_1(s) = 0.0185\frac{s+4000}{s+0.01}. \tag{10}$$

For simplicity, the weight $W_2(s)$ is chosen to be equal to $W_I(s)$, according to Eq. (7). The optimization solution is obtained using the MATLAB Robust Control Toolbox. A direct result from the MATLAB routine is a 5^{th}-order controller. Using model reduction [5], the following 3^{rd}-order robust compensator is achieved

$$G_c(s) = \frac{9.6796\cdot 10^6\,(s+1)\,(s+20.08)}{(s+3.42\cdot 10^{-3})\,(s+5.09)\,(s+3.45\cdot 10^6)}. \tag{11}$$

V Controller performance analysis and discussions

The stability and performance of the reduced 3^{rd}-order H_∞ controller, as given in Eq. (11), can be verified by examining the magnitude of $|W_2(jw)T(jw)|$ and $|W_1(jw)S(jw)| + |W_2(jw)T(jw)|$ against frequencies [5]. The results, as illustrated in Fig. 5, show that $|W_2(jw)T(jw)|$ is always smaller than 1 over the frequency range of interest, while $|W_1(jw)S(jw)|+|W_2(jw)T(jw)|$ can remain below 1 at high frequencies only. This means that the compensator $G_c(s)$ can ensure robust stability but fails to achieve robust performance. In other words, the performance specifications, i.e. the gain margin, phase margin, bandwidth of the closed loop system given in term of $W_1(s)$, are not met for some plants in the uncertainty set.

The assessments of the stability and performance for the full 5^{th}-order controller, obtained in Section IV, are carried out in a similar way. The assessment results, which have not included in this paper due to limited space, confirm that the full order compensator can guarantee robust stability but also fails in the robust performance test. The results from the stability and performance assessments for both the full and reduced order controllers reveal that both stability and performance are preserved after the model reduction.

In order to further assess the performance of the reduced order controller $G_c(s)$, a large-signal simulation of the system in Fig. 1, is used. The simulation is built based on a switched model of the flyback converter and implemented in the MATLAB/SIMULINK environment. Fig. 6 shows the simulated transient response of the flyback converter for a $0.165A$ to $3.15A$ step load and an input voltage $V_{in} = 150V$. The results from Fig. 6 confirm that the controller can bring the output voltage close to the reference level but cannot achieve zero-steady error. This result is due to the absent of the integral action in the compensator $G_c(s)$.

The output transient response in Fig. 6 is robustly stable but has a long settling time. This result can be explained in the sense that due to the huge variation in the model dynamic, as shown in Fig. 3, some performance has to be scarified in order to achieve robust stability.

VI Conclusion

This paper conducts a study of H_∞ robust control applied to a variable frequency flyback converter. The presence of the variable frequencies, in addition to the broad external disturbances, causing parametric variations, introduces another degree of variations into the plant and results in a very conservative uncertainty model which can easily fail the H_∞ synthesise procedure. The simulation results show that it is possible to design a single controller that can preserve robust stability over the whole working space of the flyback converter, but fails to maintain adequate robust performance.

References

[1] Y. Panov and M.M. Jovanovic. Adaptive off-time control for variable-frequency, soft-switched flyback converter at light loads. *IEEE Trans. Power Electron.*, 17(4):596–603, Jul. 2002.

[2] Sang Hee Kang, D. Maksimovic, and I. Cohen. Efficiency optimization in digitally controlled flyback DC-DC converters over wide ranges of operating conditions. *IEEE Trans. Power Electron.*, 27(8):3734–3748, Aug. 2012.

[3] G. Zames. Feedback and optimal sensitivity: Model reference transformations, multiplicative seminorms, and approximate inverses. *IEEE Trans. Automat. Contr.*, 26(2):301–320, Apr. 1981.

[4] K. Zhou, J. C. Doyle, and K. Glover. *Robust and Optimal Control*. Prentice Hall, Englewood Cliffs, New Jersey, 1996.

[5] S. Skogestad and I. Postlethwaite. *Multivariable Feedback Control - Analysis and Design*. John Wiley & Sons, 2001.

[6] R. Y. Chiang and M. G. Safonov. *Robust Control Toolbox User's Guide*. The Mathworks, Natic, MA, Jun. 2001.

[7] R. Naim, G. Weiss, and S. Ben-Yaakov. H_∞ control applied to boost power converters. *IEEE Trans. Power Electron.*, 12(4):677–683, Jul. 1997.

[8] A. Kugi and K. Schlacher. Nonlinear H_∞ controller design for a DC-to-DC power converter. *IEEE Trans. Contr. Syst. Technol.*, 7(2):230–237, Mar. 1999.

[9] E. Vidal-Idiarte, L. Martinez-Salamero, H. Valderrama-Blavi, F. Guinjoan, and J. Maixe. Analysis and design of H_∞ control of nonminimum phase-switching converters. *IEEE Trans. Circuits Syst. I, Fundam. Theory Appl.*, 50(10):1316–1323, Oct. 2003.

[10] Z. Q. Wang, M. Sznaier, I. Batarseh, and J. Bu. Robust controller design for a series resonant converter. *IEEE Trans. Aerosp. Electron. Syst.*, 32(1):221–233, Jan. 1996.

[11] J. Bu, M. Sznaier, Z.Q. Wang, and I. Baterseh. Robust controller design for a parallel resonant converter using μ-synthesis. *IEEE Trans. Power Electron.*, 12(5):837–853, Sep. 1997.

[12] S. Buso. Design of a robust voltage controller for a buck-boost converter using μ-synthesis. *IEEE Trans. Contr. Syst. Technol.*, 7(2):222–229, Mar. 1999.

[13] R. Tymerski. Worst case stability analysis of switching regulators using the structured singular value. In *25th Annu. IEEE Power Electron. Specialists Conf.*, volume 1, pages 281–288, Jun. 1994.

[14] G.F. Wallis and R. Tymerski. Generalized approach for μ-synthesis of robust switching regulators. *IEEE Trans. Aerosp. Electron. Syst.*, 36(2):422–431, Apr. 2000.

[15] C. Olalla, R. Leyva, A. El Aroudi, and P. Garcs. QFT robust control of current-mode converters: application to power conditioning regulators. *Int. J. of Electron.*, 96(5):503–520, 2009.

[16] O. Ojo. Robust control of series parallel resonant converters. *IEE Proc. Contr. Theory Appl.*, 142(5):401–410, Sep. 1995.

[17] G.C. Ioannidis and S.N. Manias. H_∞ loop-shaping control schemes for the buck converter and their evaluation using μ-analysis. *IEE Proc. Electric Power Appl.*, 146(2):237–246, Mar. 1999.

[18] C.A. Jacobson, A.M. Stankovic, and G. Tadmor. Design of robust controllers for resonant DC/DC converters. In *4th IEEE Conf. on Contr. Appl.*, pages 360–365, Sep. 1995.

[19] A. Altowati, K. Zenger, and T. Suntiof. Analysis and design of QFT-based robust control of a boost power converter. In *4th IET Conf. on Power Electron., Machines and Drives*, pages 537–542, Apr. 2008.

[20] R. W. Erickson and D. Maksimovic. *Fundamental of Power Electronics*. 2nd Edition, Kluwer Academic Publishers, 2004.

[21] J. Sun, D.M. Mitchell, M.F. Greuel, P.T. Krein, and R.M. Bass. Averaged modeling of PWM converters operating in discontinuous conduction mode. *IEEE Trans. Power Electron.*, 16(4):482–492, Jul. 2001.